

## The Performance of the HRIBF Recoil Mass Spectrometer

T. N. Ginter

*Department of Physics and Astronomy,  
Vanderbilt University, Nashville, TN 37235, USA  
E-mail: ginter@phy.ornl.gov*

The Recoil Mass Spectrometer (RMS) is a mass separator located at the Holifield Radioactive Ion Beam Facility (HRIBF) at Oak Ridge National Laboratory. This paper describes the RMS, its performance, its detector systems, and discusses some experiments to illustrate its capabilities.

### 1 The Recoil Mass Spectrometer

The Recoil Mass Spectrometer (RMS)<sup>1</sup> is the central component of the nuclear structure experimental end station of the Holifield facility at Oak Ridge National Laboratory. High channel selectivity is imperative in the study of nuclei far from stability. Experiments investigating these nuclei must cope with high levels of background activity that arise from scattered beam and from events in much stronger reaction channels. The RMS, together with its detector systems, provides an excellent environment for dealing with both of these sources of background; it is a powerful tool for studying exotic nuclei.

This section describes the RMS and discusses its performance. Section 2 discusses the RMS detector systems. Section 3 illustrates some of the techniques employed at the RMS by describing recent experiments.

#### 1.1 Overview of the RMS

The function of the RMS is to separate nuclei recoiling from a thin target by their mass-to-charge ratio  $A/Q$ . These nuclei are produced in fusion-evaporation reactions when a beam of heavy ions strikes the target. The RMS consists of a series of ion-optical bending and focusing elements; Figure 1 shows a schematic view of the device. The dispersion of recoils into groups by  $A/Q$  at the focal plane generally allows identification of recoils by mass; ambiguities can arise, however, because recoils with different masses and different ionic charge states can have the same value for  $A/Q$ .

The flight path through the RMS from the target position to the focal plane is 25 m. The recoil time-of-flight varies depending on the reaction but is typically on the order of 2  $\mu$ s. The size of the focal plane is 36 cm horizontally by 10 cm vertically. RMS settings can be used to adjust the size, shape, and dispersion of the mass groups. A typical size (FWHM) for the mass groups

RECEIVED  
MAR 03 1999  
OSTI

## **DISCLAIMER**

This report was prepared as an account of work sponsored by an agency of the United States Government. Neither the United States Government nor any agency thereof, nor any of their employees, make any warranty, express or implied, or assumes any legal liability or responsibility for the accuracy, completeness, or usefulness of any information, apparatus, product, or process disclosed, or represents that its use would not infringe privately owned rights. Reference herein to any specific commercial product, process, or service by trade name, trademark, manufacturer, or otherwise does not necessarily constitute or imply its endorsement, recommendation, or favoring by the United States Government or any agency thereof. The views and opinions of authors expressed herein do not necessarily state or reflect those of the United States Government or any agency thereof.

## **DISCLAIMER**

**Portions of this document may be illegible  
in electronic image products. Images are  
produced from the best available original  
document.**

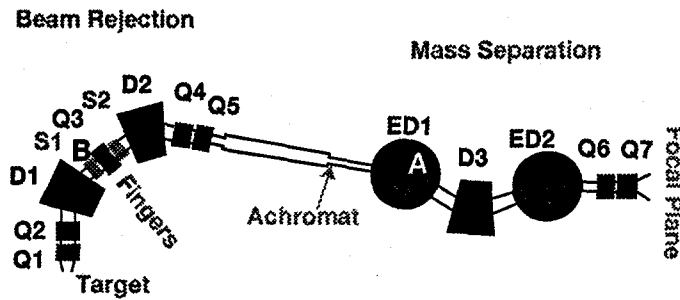


Figure 1: A schematic view of the RMS showing the positions of the magnetic quadrupoles Q1 - Q7, the magnetic dipoles D1 - D3, the magnetic sextupoles S1 and S2, and the electrostatic dipoles ED1 and ED2. The primary beam dump location for other machines is marked by "A"; "B" marks the primary beam dump for the RMS.

as measured in the symmetric reaction of a  $^{58}\text{Ni}$  beam on a  $^{60}\text{Ni}$  target <sup>2</sup>, is 1 cm wide by 2 cm high. The spacing between mass groups in this reaction was 3.5 cm, and the mass dispersion was 40 mm/‰.

The RMS elements responsible for  $A/Q$  separation are the electric-magnetic-electric dipole combination ED1-D3-ED2 (see Figure 1). This part of the device follows the same design principle as other mass separators – for example, the Fragment Mass Analyzer <sup>3</sup> at the ATLAS facility of Argonne National Laboratory and the RMS <sup>4</sup> at the Laboratori Nazionali di Legnaro in Italy. An important feature of the Oak Ridge RMS is its ability to prevent particles of the primary beam from scattering to the focal plane. The high sensitivity required for observing exotic nuclei at the focal plane depends very much on the level of beam rejection; if the detectors at the focal plane are flooded with beam events, the rare "good" events will be lost due to dead time or buried in a high background. In other machines the location where most of the beam gets dumped is marked in the Figure 1 by "A". What makes the Oak Ridge RMS unique is the extra beam rejection provided by the momentum separator near the target (magnets Q1 - Q5). For the RMS the location of the primary beam dump is after D1 and is marked in the figure by "B". Since the beam dump is farther away, scattered beam particles have much more difficulty reaching the focal plane. For especially challenging inverse reactions there is the option to use thin rods called "fingers" to block charge states of the beam which are narrowly focussed because they have a well defined momentum. These fingers, located at the momentum focal plane inside of Q3, have a minimal impact on the transmission of recoils through the device. The RMS beam suppression

makes it well suited for handling symmetric and inverse reactions where the transmission efficiency for recoils is enhanced due to kinematic focusing.

### *1.2 RMS Performance*

The RMS has an energy acceptance of  $\pm 10\%$ , an  $A/Q$  acceptance of  $\pm 4.9\%$ , and a mass resolution  $M/\Delta M$  of 450. These measured performance numbers<sup>2</sup> match the design specifications for the device.

It is not meaningful to quote a single number for the overall transmission efficiency of a recoil mass spectrometer. The transmission varies depending on the reaction kinematics (inverse or normal), the reaction channel, and the target thickness. For the specific case of a 212 MeV  $^{58}\text{Ni}$  beam on a  $500 \mu\text{g}/\text{cm}^2$   $^{28}\text{Si}$  target with a  $1 \text{ mg}/\text{cm}^2$  tantalum backing which faced the beam, a transmission efficiency of 5.2% was observed for the  $3p$  reaction channel (two charge states) and 4.1% was observed for the  $\alpha 2p$  channel (also two charge states). The important point here is that the RMS efficiency remains high even for the alpha channel. This high alpha channel efficiency results from the large RMS vertical angular acceptance and from the use of the inverse reaction.

## **2 RMS Detector Systems**

The RMS  $A/Q$  separation and beam suppression alone cannot provide the high channel selectivity necessary for studying nuclei far from stability. The high sensitivity comes from the detector systems used together with the RMS.

Presently detectors are placed at two RMS locations. The first is the target position to detect prompt radiation as the nuclei are being produced. The second location is the focal plane where the mass separated nuclei are detected by energy loss or radioactive decay.

### *2.1 Target Area Detectors*

A germanium array, CLARION (CLOver Array for Radio-active ION beams), consisting of 11 anti-Compton-shielded clover detectors, is currently being set up for doing in-beam  $\gamma$ -ray spectroscopy. Each clover consists of four germanium crystals; each crystal has a relative efficiency of about 25%. The total relative efficiency for a clover is greater than 150% with the add-back option used. The absolute photo-peak efficiency of a clover in the array for 1.33 MeV  $\gamma$ -rays is about 0.3%. Ten of the clovers have segmented electrodes to provide additional position resolution. Although the array is not yet fully in place, six of the clovers (without anti-Compton shielding) have been used for experi-

ments over the past year. An array of charged particle detectors – similar to the Microball system<sup>5</sup> used with GAMMASPHERE – is also under development.

### *2.2 Focal Plane Detectors*

The detector configurations used at the focal plane usually employ a position sensitive avalanche counter (PSAC), which detects the spatial separation of nuclei by  $A/Q$  produced by the RMS. An ionization chamber may be placed behind the PSAC to provide  $Z$ -identification of the recoils within a mass group based on their energy loss. The ion chamber is large enough to accept all of the mass groups entering the PSAC. Alternatively, a double-sided silicon strip detector (DSSD)<sup>6</sup> may be placed behind the PSAC to study alpha or proton emissions from implanted recoils. The DSSD is large enough to accept one or two mass groups. A moving tape collector may also be placed behind the PSAC to accept one of the mass groups. Movements of the tape are used either to transport the activity of the implanted recoils to a detector station away from the focal plane or to prevent long-lived activity from building up in front of the detector station. E. F. Zganjar describes the moving tape collector and the detector setups that can be used with it in a separate contribution to these proceedings.

## **3 Experimental Techniques Used with the RMS**

The challenge presented by the study of nuclei far from stability is the extremely low cross-section with which they are produced compared to other reaction channels. This section describes some of the techniques used to combine the RMS with its detector systems to achieve the high sensitivity required to select exotic nuclei from others produced in the reactions.

### *3.1 Recoil- $\gamma$ with Ionization Chamber $Z$ -Identification*

One technique involves using the germanium array at the target position together with the PSAC and ionization chamber at the focal plane. The PSAC and ionization chamber provide  $A/Q$  and  $Z$  identification of recoils for tagging the gamma rays observed at the target.

This technique was used to provide the identification of prompt  $\gamma$ -rays in the  $N = Z + 1$  nucleus  $^{79}_{39}\text{Y}_{40}$ .<sup>7</sup> This nucleus was produced using the reaction  $^{28}\text{Si}(\text{Fe},p2n)^{79}\text{Y}$ . Figure 2(a) contains a plot illustrating the ionization chamber performance. Gating on the energy loss observed in the ionization chamber for the mass 79 recoils allows one to obtain spectra with the enhanced presence of  $\gamma$ -rays from the different mass 79 isotopes. It is then possible to obtain

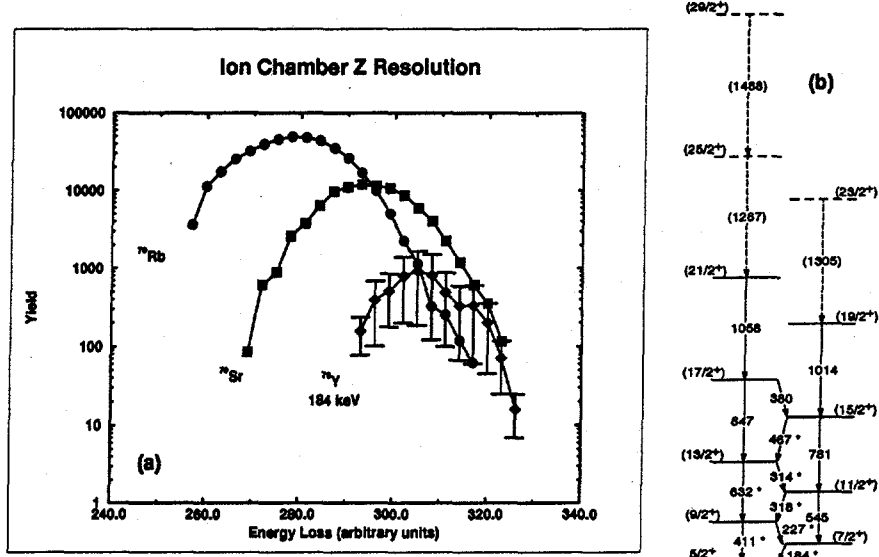


Figure 2: (a) Ionization chamber energy loss spectrum for mass 79 recoils obtained by gating on known  $\gamma$ -rays in <sup>79</sup>Rb and <sup>79</sup>Sr and on the newly identified 184 keV  $\gamma$ -ray in <sup>79</sup>Y. (b) New level scheme for <sup>79</sup>Y from the RMS experiment together with an earlier GAMMASPHERE experiment. The transitions marked by “\*\*” were observed in the RMS experiment.

a “clean” gamma spectrum for each of the isotopes by doing an appropriate background subtraction. The new level scheme for <sup>79</sup>Y, shown in Figure 2(b), was constructed based on the RMS data together with data from an earlier GAMMASPHERE experiment that did not employ a mass separator. The transitions marked by “\*\*” were observed in the RMS experiment and could be uniquely assigned to <sup>79</sup>Y. Using the GAMMASPHERE experiment alone, it would have been difficult to pull this level scheme out of the data and impossible to assign it unambiguously to <sup>79</sup>Y. The main result of the <sup>79</sup>Y study is that proton-neutron correlations, which are expected to be important for  $N \sim Z$  nuclei in this region, did not need to be invoked explicitly in theoretical models to adequately describe the data.

### 3.2 Charged Particle Decay Studies Using a DSSD

Another class of experiments involves using the DSSD placed behind the PSAC for proton emission studies. The size of the DSSD is 4 cm by 4 cm. The

DSSD consists of 40 horizontal strips positioned in front of 40 vertical strips to provide 1600 individual pixels for detecting recoil implantation events and their subsequent decay by alpha or proton emission. The large number of pixels means that it is possible to look for the decay of an implanted ion on a comparatively long time scale before a new ion gets implanted into the same pixel. (This time scale, of course, depends on the overall rate at which recoils are implanted into the DSSD.) These experiments are discussed by C. R. Bingham in a separate contribution to these proceedings.

### 3.3 Recoil Decay Tagging

The DSSD (behind the PSAC) can also be coupled to the germanium array at the target. This arrangement makes it possible to use the known alpha or proton decay of an exotic nucleus observed at the focal plane to correlate with prompt gamma rays observed at the target. This technique is known as recoil decay tagging (RDT).<sup>8</sup>

This setup was used to identify  $\gamma$ -rays in  $^{151}\text{Lu}$  using the ground state proton radioactivity.<sup>9</sup> This nucleus was produced using the reaction  $^{96}\text{Ru}(^{58}\text{Ni}, p2n) ^{151}\text{Lu}$  with a beam energy of 266 MeV. Figure 3(a) shows the  $\gamma$ -rays observed in coincidence with the mass 151 recoils at the focal plane. Figure 3(b), obtained by the further requirement that a proton from the decay of  $^{151}\text{Lu}$  be present (with a background subtraction to eliminate randomly correlated events, shows the  $\gamma$ -ray spectrum belonging to  $^{151}\text{Lu}$ . This is the first time that  $\gamma$ -rays from this nucleus have been observed. An open question left by the this experiment is whether the observed prompt transitions feed the ground state or an isomeric state which may be expected on the basis of energy level systematics in neighboring nuclei.

### 3.4 Microsecond Isomer Spectroscopy

Another way to extract information about exotic nuclei is to use  $\gamma$ -decaying microsecond isomers observed with clover detectors placed behind the PSAC at the focal plane. These isomers live long enough to survive the flight time (typically a couple of microseconds) through the RMS. One option is to perform spectroscopy on the decay of these isomers. A clean spectrum of the isomeric decay is obtained by recording the  $\gamma$ -rays occurring within a time window of a few tens of microseconds after the arrival of the recoil at the focal plane. This technique has been used, for example, with the velocity filter SHIP at GSI to study<sup>10</sup> the decay of the  $3.2 \mu\text{s}$  isomer in  $^{76}\text{Rb}$ . In cases where the  $\beta$ -decay of an isotope feeds a known microsecond  $\gamma$ -decaying isomer, the  $\gamma$ -rays can be used as a unique tag to study the  $\beta$ -decay. The half-life of  $^{80}\text{Zr}$  was measured

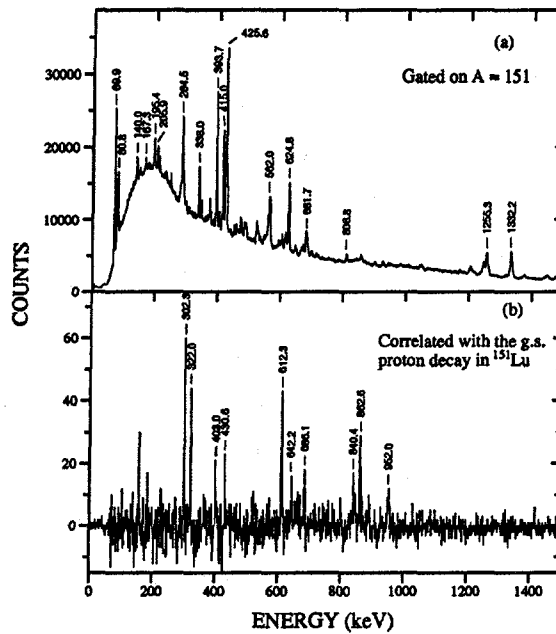


Figure 3: Data from the  $^{151}\text{Lu}$  RDT experiment performed at the RMS. (a) Prompt  $\gamma$ -rays correlated to mass 151 recoils reaching the focal plane. (b) Prompt  $\gamma$ -rays correlated to the ground state proton emission of  $^{151}\text{Lu}$  observed at the focal plane

at the RMS<sup>11, 12</sup> using this technique. Another way to make use of a known  $\gamma$ -decaying isomer is to tag prompt  $\gamma$ -rays feeding the isomer observed at the target position as in RDT.

A variety of detector setups can be used depending upon the exact nature of the experiment. The choice between using the moving tape collector or a simple catcher chamber is dictated by the trade-off between the need to remove long-lived activity and the need to maximize detection efficiency by packing more detectors closer to the collection point. The kinds of detectors we have used around the collection point include clover detectors with and without their anti-Compton shields and X-ray detectors.

The case of the  $N = Z$  nucleus  $^{66}\text{As}_{33}$  is one example that illustrates the power of isomer spectroscopy at the RMS. This isotope has two isomers with half-lives of 17 and 1.9  $\mu\text{s}$ . They were first identified and studied in a fragmentation experiment at GANIL.<sup>13</sup> Fragmentation experiments have the advantage that the isomeric  $\gamma$ -rays observed can be assigned unambiguously to a given isotope. However, because  $^{66}\text{As}$  is the only nucleus with any microsec-

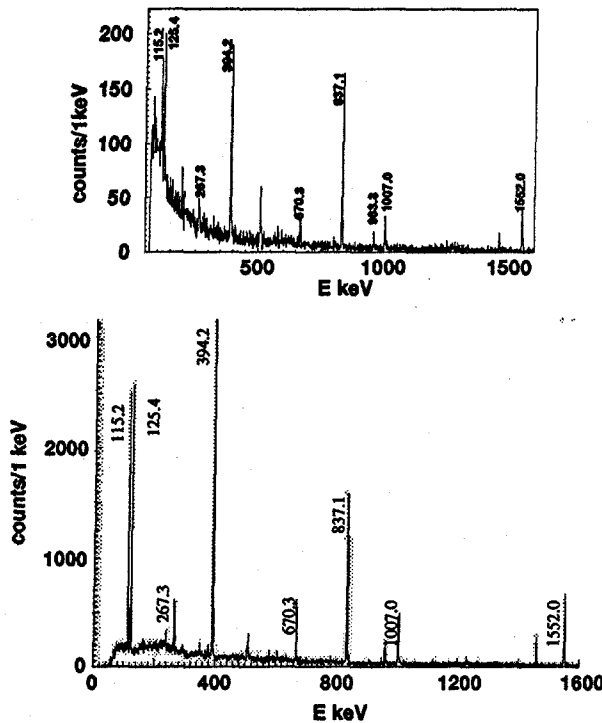


Figure 4: Top: The  $\gamma$ -ray energy spectrum observed within  $\sim 40 \mu\text{s}$  of implantation of  $^{66}\text{As}$  fragments during a 96 hour run at GANIL. Bottom: The  $\gamma$ -ray energy spectrum observed within  $\sim 20 \mu\text{s}$  of implantation of mass 66 recoils during a 10 hour run at the RMS. Labeled peaks are known  $^{66}\text{As}$  transitions.

ond isomers in the  $A = 66$  mass chain, the RMS mass separation provides completely clean conditions for studying these isomers as is illustrated in Figure 4. In this instance the overall count rate obtained with fusion-evaporation at the RMS is about a factor of ten higher than with fragmentation. The case of  $^{66}\text{As}$  is a good example of where the isomeric  $\gamma$ -rays observed at the focal plane may be used as a tag to identify the correlated prompt  $\gamma$ -rays at the target position.

#### 4 Summary

The RMS is a highly effective tool for detailed spectroscopic investigations of nuclei far from stability. The powerful RMS detector systems combine with the excellent RMS performance to minimize background and to maximize channel

selectivity. The following are among the techniques that have been successfully applied to nuclear structure studies so far at the RMS:

- proton emission studies
- recoil- $\gamma$  studies with ionization chamber  $Z$ -identification
- recoil decay tagging (RDT)
- $\gamma$ -decaying isomer and  $\beta$ -decay studies

### Acknowledgments

Oak Ridge National Laboratory is managed by Lockheed Martin Energy Research Corp. for the U. S. Department of Energy under contract No. DE-AC05-96OR22464.

### References

1. J. D. Cole, *et al.*, *Nucl. Instrum. Methods B* **70**, 358 (1992).
2. C. J. Gross, *et al.*, *Application of Accelerators in Research and Industry*, AIP Conf. Proc. No. 392 (AIP, Woodbury, NY, 1997), Vol. 1, p. 401.
3. C. N. Davids and J. D. Larson, *Nucl. Instrum. Methods B* **40/41**, 1224 (1989).
4. P. Spolaore, *et al.*, *Nucl. Instrum. Methods A* **238**, 381 (1985).
5. D. G. Sarantites, *et al.*, *Nucl. Instrum. Methods A* **381**, 418 (1996).
6. P. J. Sellin, *et al.*, *Nucl. Instrum. Methods A* **311**, 217 (1992).
7. S. D. Paul, *et al.*, *Phys. Rev. C* **58**, R3037 (1998).
8. E. S. Paul, *et al.*, *Phys. Rev. C* **51**, 78 (1995).
9. C.-H. Yu, *et al.*, *Phys. Rev. C* **58**, R3042 (1998).
10. S. Hofmann, *et al.*, *Z. Phys. A* **325**, 37 (1986).
11. J. Ressler, *et al.*, to be published.
12. A. Piechaczek, contribution to these proceedings.
13. R. Grzywacz, *et al.*, *Phys. Lett. B* **429**, 247 (1998).